Ring Fault and Caldera Formation: Insights Provided by Three-Dimensional Elastic Finite Element Models.
R.T. Goldman[1], J.A. Albright[1], and E.B. Grosfils[1], [1]Pomona College, Claremont, CA (egrosfils@pomona.edu).

Introduction: Caldera eruptions are among the most destructive [1] but least understood [2] volcanic events on Earth. The most powerful caldera "supereruptions" only occur every 100,000 years or so [1], but as populations continue to expand and encroach upon areas that could be directly affected by a caldera-forming eruption (e.g., at Long Valley, California, at Campi Flegrei, Italy, or at Rabaul, Papau New Guinea [2]) there is ample motivation to improve our insight into the mechanics of ring fault formation and caldera development. Studying the process of caldera formation can also help explain the origin of these features on other terrestrial planets, including Venus and Mars, and on moons such as Io [3].

Quantitative models of a magma reservoir embedded in an elastic host are regularly used to learn more about volcanic systems such as those that form calderas [4-11]. While useful, most of these models employ either axisymmetric geometries or vertical two-dimensional slices, imposing geometric limitations. In this study we seek new insight into the mechanics of ring fault initation and caldera formation by developing, testing and applying fully three-dimensional (3D) elastic finite element models. Here we briefly describe the model and report selected initial results pertaining to tectonic stress effects; related studies are ongoing.

Methods: Using COMSOL Multiphysics, we designed 3D elastic finite element models to assess ring fault formation. The first modeling goal is to identify locations where Mohr-Coulomb (MC) and tensile failure initiate for inflating ellipsoidal reservoirs of varying geometry and depth, and to quantify the overpressure required. A second objective is to determine if horizontal tectonic stresses modify the failure characteristics, and to assess the implications for ring fault initiation and geometry when compared to otherwise identical cases with no tectonic stress applied.

Calibration. To test the model we initially create 3D reservoir geometry and loading conditions that duplicate those used in axisymmetry studies [8]. The 3D models successfully reproduce: the distribution of stress contours near the reservoir; the dependence of tensile failure location on reservoir depth, geometry, tensile strength and magma density; and, the overpressure required to induce tensile failure. We also duplicate published [11] and unpublished axisymmetric MC failure results successfully, and conclude that the behavior of the reservoir and surrounding host is captured accurately by our 3D model formulation.

Results and Discussion: Following [11] we use the $A\psi$ parameter of [12] to depict Andersonian fault regimes within the host rock volume (Fig 1). During inflation, rock stress near the reservoir favors either concentric thrust faults (red) or concentric normal faults (green). Next, we identify areas where the Andersonian fault type and steepest concentric (most ring fault like) MC fault plane alignment agree (Fig 1). Finally streamlines, seeded only in zones where MC failure has occurred, help reveal the connectivity between local MC fault planes, i.e. their 3D geometry. If the streamlines remain within areas where $A\psi$ and the local MC fault plane alignment agree, and if their geometries mimic ring fault geometries seen in the field, then we conclude the host rock is primed for ring faulting (Fig 2a). Conversely, if MC streamlines propagate beyond the zone where $A\psi$ and MC fault plane alignments agree, we conclude that the system is not well primed for ring fault formation and slip (Fig 2b).

When compared to benchmarks with no regional stress, tectonic extension reduces the overpressure required to initiate both MC and tensile rupture significantly; these differences are more pronounced at shallow depth. In contrast, tectonic compression has almost no effect (Fig 3). Regional extension thus enhances tensile rupture conditions and, since resulting intrusions relieve magma pressure in the reservoir, it also reduces the likelihood that significant zones of MC failure (where ring faults might nucleate) can develop before tensile failure and intrusion occur.

Application of regional stresses also affects the geometry of the zone where MC plane alignments and $A\psi$ agree. When subjected to compression, for example, the area primed for ring faulting preferentially extends upward along planar zones parallel to the axis of compression (Fig. 4). This creates the potential to produce partial annuli, if the system arrests, like those observed in places on Venus [13]. A less vertically extensive zone of agreement circling the reservoir (Fig. 4), however, suggests another possible outcome: faults propagating to the surface locally may trigger “unzipping” to form a 360° ring fault, as has been documented at some calderas on Earth (e.g., Long Valley [14]).

From the initial results reported here, we conclude that the 3D model formulation described can yield new insight into planetary ring fault and caldera formation. Ongoing modeling efforts will continue building upon these results and are expected to improve our knowledge of related volcanological phenomena.

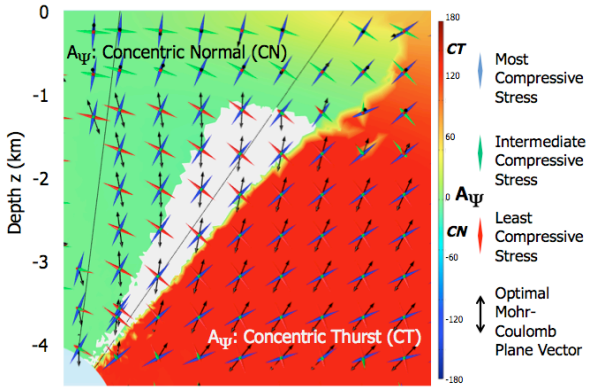

Figure 1: *Principal stress orientations above a spherical 5 km deep magma reservoir. Colors depict Aψ parameter quantifying stress regime. White area shows where Aψ and concentric MC plane alignments agree.*

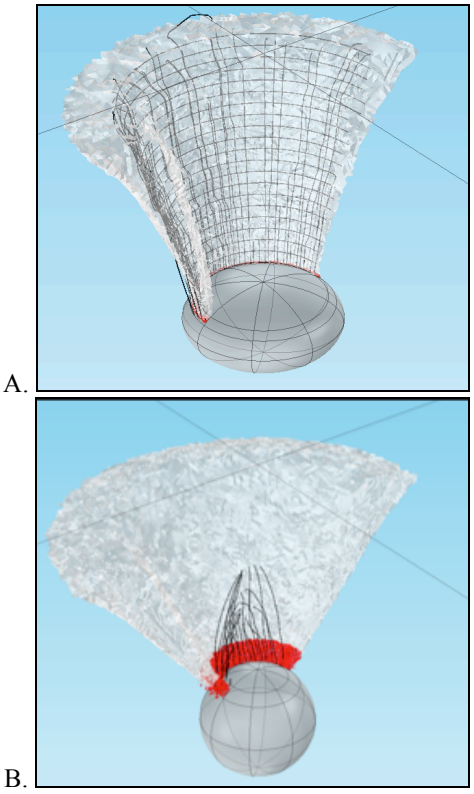

Figure 2: (a) *Conical zone of potential ring faulting above an oblate reservoir in the absence of tectonic stress (half of cone omitted for visualization clarity). Volume where host rock stress regime and MC fault planes agree (white) contains MC planes (streamline crosshatch) seeded in zone of MC failure (red) at reservoir wall. This oblate reservoir is primed for ring fault formation.* **(b)** *In contrast, this spherical reservoir is not primed for ring faulting since MC plane streamlines do not remain within the white volume denoting the host rock region suitably primed for ring fault slip.*

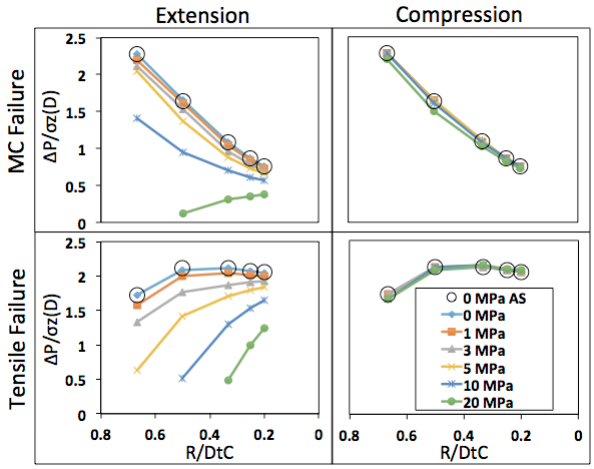

Figure 3: *Magma overpressures required to reach MC (top) and tensile (bottom) failure of a spherical reservoir as a function of the reservoir radius-to-depth ratio for several values of tectonic extension (left) and compression (right). Hollow black circles are data obtained from axisymmetric models with the same parameters as 3D models with no tectonic stress applied.*

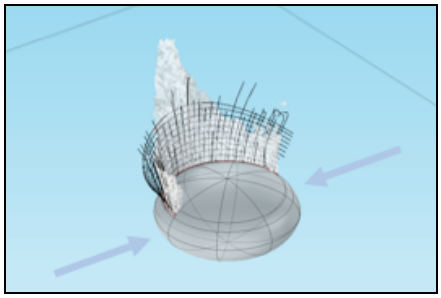

Figure 4: *During compression, narrow zone primed for ring faulting forms parallel to the compression axis (purple arrows). It remains linked to a fully annular, less vertically extensive zone by the reservoir.*

References: [1] Gregg P.M. et al. (2012) *JVGR, 241-242,* 1-12. [2] Newhall C.G. & Dzurisin D. (1988) *USGS Bull, 1855.* [3] Kieffer S.W. (1995) *Science, 269,* 1385-1391. [4] Anderson E.M. (1936) *Proc Royal Soc Edin, 56,* 128-157. [5] Mogi, K. (1958) *Bull Earthquake Res Inst, Univ Tokyo, 36,* 99-134. [6] McTigue D.F. (1987) *JGR, 92,* 12931-40. [7] Zuber M.T. & Mouginis-Mark, P.J. (1992) *JGR, 97,* 18295-307. [8] Grosfils E.B. (2007) *JVGR, 166,* 47-75. [9] Long S.M. & Grosfils E.B. (2009) *JVGR, 186,* 349-360. [10] Gudmundsson, A. (2012) *JVGR, 237-238,* 19-41. [11] Grosfils E.B. et al. (2013) *GSL Spec Pub, 401.* [12] Simpson R.W. (1997) *JGR, 102,* 17909-19. [13] Roberts K.M. & Head J.W. (1993) *GRL, 20,* 1111-14. [14] Hildreth W. & Mahood G.A. (1986) *GSA Bull, 97,* 396-403.